Partial Oxidation of Methane to Syngas via Formate Intermediate Found for a Ruthenium-Rhenium Bimetallic Catalyst

*Lingcong Li, Nazmul H. MD Dostagir, Abhijit Shrotri, Atsushi Fukuoka, Hirokazu Kobayashi**

Institute for Catalysis, Hokkaido University, Kita 21 Nishi 10, Kita-ku, Sapporo, Hokkaido 001-0021, Japan.

Email: kobayashi.hi@cat.hokudai.ac.jp

ABSTRACT Partial oxidation of methane (POM) is a potential technology to increase the efficiency of synthesizing a mixture of CO and H_2 named syngas, compared to steam reforming processes. Recently, supported metals modified with Re emerged as active catalysts for POM. However, roles of Re in this reaction has been unclear. Here, we demonstrate that the addition of Re to Ru/Al_2O_3 catalyst changes the reaction mechanism. The bimetallic catalyst oxidizes CH_4 to mainly CO *via* formate. After using all O_2, steam reforming and reverse water-gas shift take place to increase the yield of CO and H_2. This is in contrast to Ru/Al_2O_3, which catalyzes POM mostly by complete oxidation of CH_4 to CO_2 and H_2O and subsequent reforming reactions. In the bimetallic catalyst, the main role of Ru is to reduce Re species, and the reduced Re species produces formate from CH_4 and also accelerates the steam reforming reaction. The dual roles of

Re increase the total catalytic performance. These results show that Re is a main player rather than a simple promoter in the catalytic reaction.

KEYWORDS Methane, bimetallic catalyst, rhenium, partial oxidation, formate

Introduction

Methane (CH_4), the main component of natural gas, shows increasing attention in chemical industries, as it can be converted to fundamental chemical products such as methanol, olefins, Fischer-Tropsch (FT) oil, and acetic acid.[1-5] Syngas is a mixture of CO and H_2 that is a common intermediate to manufacture the above mentioned chemicals.[6, 7] Steam reforming of CH_4 (SRM, eq. 1) and its modified processes have been implemented to produce syngas for a long time.[8, 9] However, SRM is an endothermic reaction operated at a temperature above 800 °C, which results in large energy consumption and high cost. Alternatively, partial oxidation of methane (POM) to syngas (formally eq. 2) is a potentially efficient method to reduce energy consumption.[10-15]

$$CH_4 + H_2O \rightleftarrows CO + 3H_2, \quad \Delta H°_{298\,K} = +206\ \text{kJ mol}^{-1} \qquad (1)$$

$$CH_4 + 1/2O_2 \rightarrow CO + 2H_2, \quad \Delta H°_{298\,K} = -36\ \text{kJ mol}^{-1} \qquad (2)$$

Rh,[11, 16-20] Ru,[21-25] Pd,[22, 26-28] Pt,[29-30] and Ni[31-37] have been mainly investigated as active catalysts for the POM reaction in the past years. Most of supported metal catalysts need a temperature of 700 °C or higher in the reaction,[10] but the reaction temperature below 650 °C is suitable to enable the use of inexpensive stainless steel reactors. Facing the challenge, doping of promoters is an approach for improving the activity.[22, 28, 38-44] Recently, Re has emerged as an additive to supported metal catalysts to improve the activity in POM at relatively low temperatures.[45,46] For example, 10 wt% Ni/Al_2O_3 catalyst gives 28% conversion of CH_4 and 16% yield of CO at 600 °C, while 7 wt% Ni-3 wt% Re/Al_2O_3 provides 100% conversion of CH_4 and 45% yield of CO under the same reaction conditions.[46] Re may increase the dispersion of

supported metals,[46] but no work has clarified the role of Re to achieve the improved performance so far.

To understand the unknown roles of Re, we summarize general reaction pathways for POM. The reaction can be classified into two categories. The first one is an indirect pathway that contains complete combustion of CH_4 to CO_2 and H_2O (eq. 3) and subsequent SRM (eq. 1) and reverse water-gas shift reaction (RWGS; eq. 4).[47, 48] In this case, SRM and RWGS are controlled by thermodynamic equilibrium. A characteristics for this pathway is almost no formation of CO or H_2 in the presence of O_2, because the oxidant suppresses the steam reforming and RWGS.[22, 49, 50] Most of catalysts follow the indirect pathway. The other is the direct partial oxidation (ideally eq. 2), where neither CO_2 nor H_2O is an intermediate.[51] Instead, a possible intermediate is atomic carbon generated by the dehydrogenation of CH_4, and the species combines with a surface adsorbed O species to form CO.[51] The direct partial oxidation pathway should produce CO or H_2 in the presence of O_2. Therefore, the two pathways are distinguishable by the product selectivity under the oxidizing ambient. The direct pathway is more attractive than the indirect one because the reaction result can be changed by kinetics and detailed mechanism. Re may promote some of these steps or possibly changes the reaction pathway.

$$CH_4 + 2O_2 \rightarrow CO_2 + 2H_2O,\ \Delta H^\circ_{298\ K} = -890\ kJ\ mol^{-1} \quad (3)$$

$$CO_2 + H_2 \rightleftarrows CO + H_2O,\ \Delta H^\circ_{298\ K} = +41\ kJ\ mol^{-1} \quad (4)$$

In this work, we propose that Re creates a direct partial oxidation pathway via formate in addition to promoting SRM and RWGS. Our work initially develops a bimetallic Ru-Re/Al_2O_3 catalyst that shows high activity in POM at 600 °C. Characterization and control experiments using the catalyst indicate that Ru reduces Re species to make it active, rather than direct

concerted effects. The Re species produces a formate intermediate from CH_4, and subsequent decomposition of the intermediate produces CO. This is a direct partial oxidation mechanism different from that passes through atomic C. In contrast, Ru/Al_2O_3 mostly follows the indirect pathway. After the direct partial oxidation using O_2, SRM and RWGS start on the bimetallic catalyst in the absence of O_2.

Experimental Section

Bimetallic Ru-Re catalysts were prepared as follows: NH_4ReO_4 (0.0216 g, 99.9%, Sigma-Aldrich Co., Ltd.) and $RuCl_3 \cdot nH_2O$ aq. (4.87 mmol L^{-1}, 10.16 mL, Wako Pure Chemical Industries) were dissolved in 15 mL of deionized water and stirred for a few minutes, and then 0.48 g of Al_2O_3 (JRC-ALO-8, Catalysis Society of Japan (CSJ)) was added into the solution. The mixture was stirred using a magnetic spin bar (700 rpm) at room temperature for 24 h, and evaporated at 50 °C under a decreased pressure (80 hPa) using a diaphragm pump. The resulting powder was dried in air at 110 °C overnight, heated to 500 °C by 5 °C min^{-1}, and afterward kept at the temperature for 5 h to obtain the catalyst named $Ru\text{-}Re/Al_2O_3$. The loading amounts of Ru and Re were 1 wt% and 3 wt%, respectively, which was confirmed by an energy dispersive X-ray analysis (Shimadzu, EDX-720) using an absolute calibration method. The same procedure was adopted for other supports, SiO_2 (JRC-SIO-9A, CSJ), MgO (JRC-MGO-4-500A, CSJ), ZrO_2 (Wako, 264-01482), and CeO_2 (Kanto, 07167-23). Ru/Al_2O_3 and Re/Al_2O_3 catalysts were obtained by the same method except for using only one metal source.

The POM was performed in a vertical quartz fixed-bed flow reactor (i.d. = 7 mm). The temperature inside of the catalyst bed was monitored by a thermocouple (ø0.5 mm) protected in a

quartz tube (ca. ø2 mm), which indicated increase in temperature was less than 20 °C during POM. A catalyst (20 mg) was put on quartz wool (Tosoh, Fine grade) in the middle of the reactor. The reactor set in an electric tube furnace (Asahi Rika, ARF-30KC) was heated to a designated temperature under N_2 flow (9.2 mL min^{-1}), followed by the introduction of a gas mixture (typically, CH_4 10.0 mL min^{-1}, O_2 0.8 mL min^{-1}, N_2 9.2 mL min^{-1}). Products were analyzed by an on-line gas chromatograph (Shimadzu GC-8A) equipped with a thermal conductivity detector (TCD) and Molecular Sieve 5A and Shincarbon ST columns to analyze N_2, O_2, CH_4, CO, and CO_2. Amounts of products were quantified by an internal standard method using N_2, by which we found that error in carbon balance was below 2.5%. H_2 was analyzed by another GC equipped with a Molecular Sieve 5A column using Ar carrier. We defined conversion of CH_4 and yields of products as eqs. 5 and 6, to increase their accuracy especially at a low conversion of CH_4. In the equations, n_x shows the amount of compound x determined by GC analysis. This treatment is justified because of no formation of other carbon-containing products except for trace carbon (<0.1% yield).

$$\text{Conversion of } CH_4 = \frac{n_{CO} + n_{CO_2}}{n_{CH_4} + n_{CO} + n_{CO_2}} \times 100\% \quad (5)$$

$$\text{Yield of CO and } CO_2 = \frac{n_{CO \text{ or } CO_2}}{n_{CH_4} + n_{CO} + n_{CO_2}} \times 100\% \quad (6)$$

Details for other experiments are summarized in Supporting Information.

Results and Discussion

POM performance of the prepared catalysts

We prepared Ru/Al_2O_3, Re/Al_2O_3, and $Ru\text{-}Re/Al_2O_3$ catalysts, where the content of Ru was 1 wt% and that of Re was 3 wt%. Effects of metal loading amounts and supports on POM are shown in Supporting Information (Figures S1−S3 and Table S1). For the bimetallic catalyst, in X-ray diffraction (XRD) analysis, Ru species was present as RuO_2 particles with 20 nm in size determined by the Scherrer equation, and Re species were not visible (Figure 1a). A high-angle annular dark-field scanning transmission electron microscopy (HAADF-STEM) measurement with EDX analysis displayed that Re species were highly dispersed with an average size of 0.5 nm (Figure 1c; more details in Figures S4a–c). Oxidation state of the Re species was nearly 7+ in average, based on the white line area of Re L3-edge X-ray absorption near-edge structure (XANES; Figure 1e).[52] The peak area correlates with the unoccupancy of 5d orbitals of Re, thus reflecting the oxidation state.

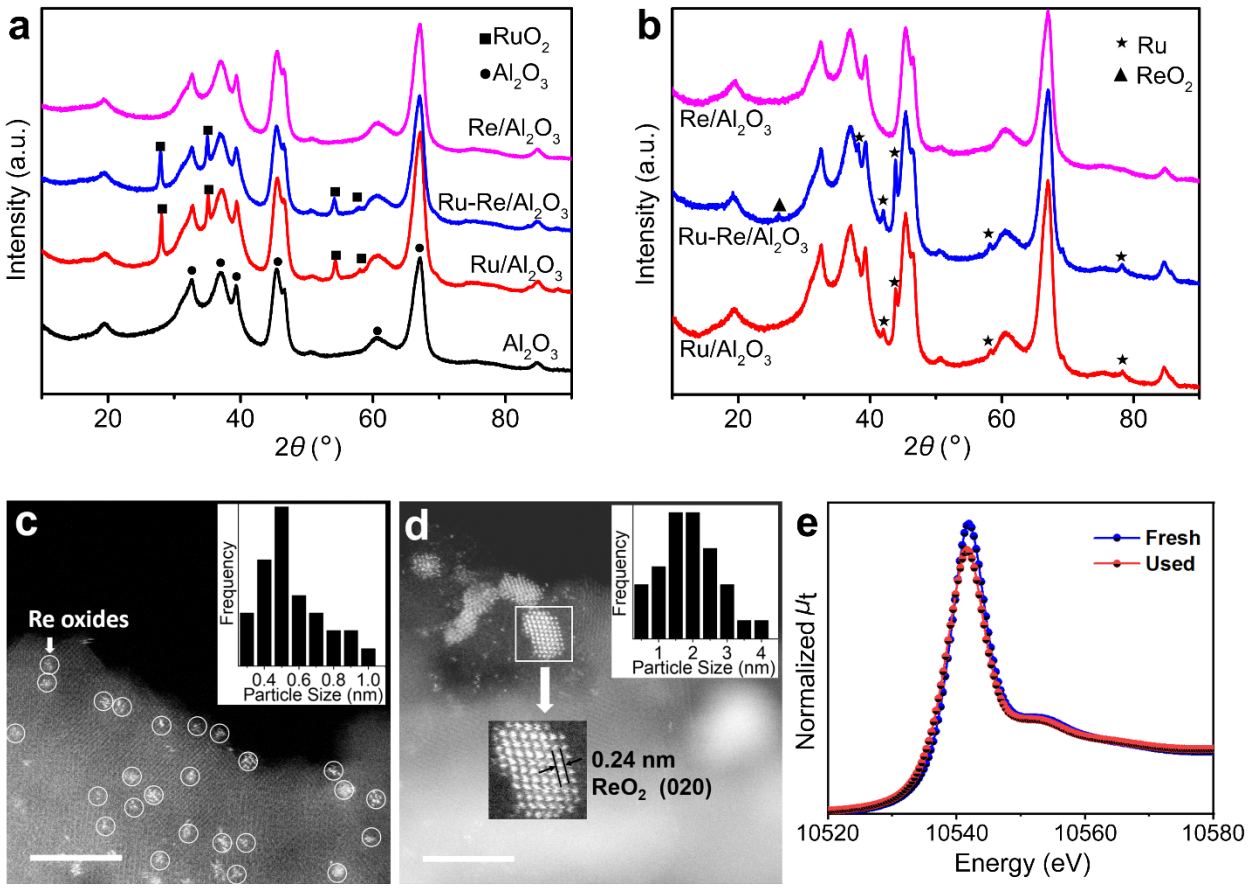

Figure 1. Characterization of catalysts. XRD patterns of (a) fresh catalysts and (b) used ones after POM at 600 °C for 3 h. (c) HAADF-STEM image and particle size distribution of Re species for fresh Ru-Re/Al_2O_3, and (d) those for the spent catalyst. The scale bars in (c) and (d) show 5 nm. (e) Re L3-edge transmission XANES spectra for fresh and the used Ru-Re/Al_2O_3.

The POM was performed at 600 °C using a gas mixture of $CH_4/O_2/N_2$ = 50/4/46 at a space velocity (SV) of 60,000 mL g^{-1} h^{-1}. The CH_4-rich condition (O_2/CH_4 = 0.08) is useful to evaluate the stability of catalyst whether it causes coke deposition. Figure 2a shows the catalytic performance at 1 h after starting the reaction. Ru-Re/Al_2O_3 gave 13% yield of CO (selectivity 93%) and 13% yield of H_2 (sel. 94%) with 100% conversion of O_2. This result is as good as that

given by one of the most active catalysts ever reported (Rh/MOR; CO 14% yield, 92% sel. under the same conditions except for SV = 6,000 mL g^{-1} h^{-1})[50] despite the 10-times higher SV. In control experiments, Ru/Al_2O_3 gave lower yields of CO (6%) and H_2 (8%), and the Re-only catalyst showed low activity (CO 1.2% yield). Note that Re/Al_2O_3 produced CO in the presence of residual O_2 (O_2 conv. 45%), which is important to understand the role of Re (see sections for the mechanistic study). These results clearly show the synergy between Ru and Re for POM. Ru-Re/Al_2O_3 increased the yield of CO and H_2 up to 54% and 61% with slightly decreased selectivity at increased O_2/CH_4 ratios (Figure 2b and Table S2). Clearly, Ru-Re/Al_2O_3 catalyst is very active for POM at a temperature as low as 600 °C.

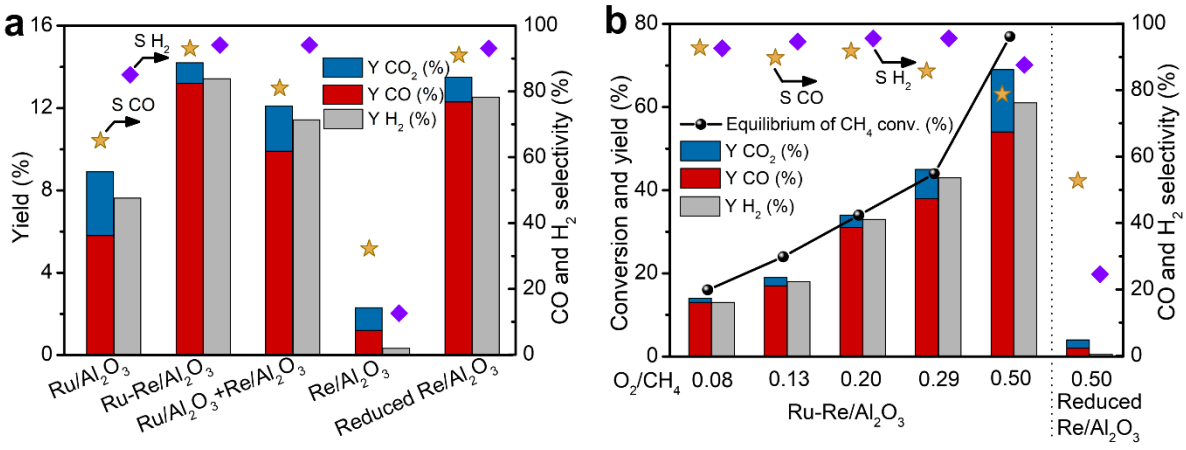

Figure 2. POM at 600 °C with a space velocity (SV) of 60,000 mL g^{-1} h^{-1}. (a) CH_4: O_2: N_2 = 50:4:46. (b) Catalysts were Ru-Re/Al_2O_3 and reduced Re/Al_2O_3, and concentration of O_2 was kept at 4% when changing O_2/CH_4 ratio. The data were sampled at 1 h after starting the reactions.

To reveal the bimetallic effect, a 1:1 physical mixture of Ru/Al_2O_3 and Re/Al_2O_3 was tested under the same reaction conditions. As we kept the same SV of 60,000 mL g^{-1} h^{-1}, amounts of Ru and Re corresponded to half of those in other tests. Nonetheless, activity of the physically

mixed catalyst (CO 10% yield; Figure 2a Ru/Al_2O_3+Re/Al_2O_3) was better than that of Ru/Al_2O_3 (6%). Ru and Re show synergy even when they are distant from each other. For their possible roles, we speculate that Ru converts CH_4 to CO and H_2 to some extent as indicated by the activity of Ru/Al_2O_3, and the produced H_2 reduces Re species. The reduced Re species might be active for POM reaction. The reduction of Re was evidenced by Re L3-edge XANES measurement of Ru-Re/Al_2O_3 catalysts before and after POM. Specifically, the used Ru-Re/Al_2O_3 represented a decreased intensity of white line, 93% compared to that of the fresh catalyst (Figure 1e), even after exposed to air at room temperature.

If the major role of Ru is the reduction of Re, reduced Re/Al_2O_3 should work for POM without Ru. As a result, reduced Re/Al_2O_3 was indeed active in the absence of Ru, but Ru was needed to keep the reduced state of Re as follows: Re/Al_2O_3 reduced with H_2 gave 12% yield of CO under the methane-rich reaction conditions (O_2/CH_4 = 0.08; Figure 2a), which was almost the same catalytic performance as that of Ru-Re/Al_2O_3. The Re catalyst largely decreased the activity (CO 2.1% yield; 53% selectivity) under the stoichiometric condition (O_2/CH_4 = 0.5) due to re-oxidation of Re (Figure 2b). The main role of Ru is the reduction of Re species to make it active in our case. Additionally, it is notable that O_2 conversion was 15% in the reaction over Re/Al_2O_3 under the stoichiometric condition, which also represents that Re produces CO in the presence of O_2.

We have also found that Ru proactively facilitates the reduction of Re in Ru-Re/Al_2O_3 catalyst in temperature-programmed reduction (TPR) experiments (Figure 3). Re species on Re/Al_2O_3 was reduced at 459 °C, and the peak completely shifted to a lower temperature (416 °C) for Ru-Re/Al_2O_3. Re species are dispersed on the support and not always close to Ru

particles as observed by STEM (Figures 1c, S4), but the reduction is enhanced by Ru. This result suggests a hydrogen spillover mechanism. Ru produces active hydrogen species and they spill over the support to reduce Re species distant from Ru. Choi *et al.* have revealed that Al-rich oxide supports easily cause hydrogen spillover.[53] Moreover, we have demonstrated a similar phenomenon for the combination of Co and Rh in a previous study, where spillover hydrogen produced by Rh assists the reduction of CoO_x.[12] Accordingly, the co-impregnation of Re and Ru is better than the physical mixture of individual Ru and Re catalysts, to maximize the reduction effect. Consumed amount of H atom was an H/Re atomic ratio of only 1.2 in the TPR, suggesting that slight reduction of Re greatly affects the catalytic activity.

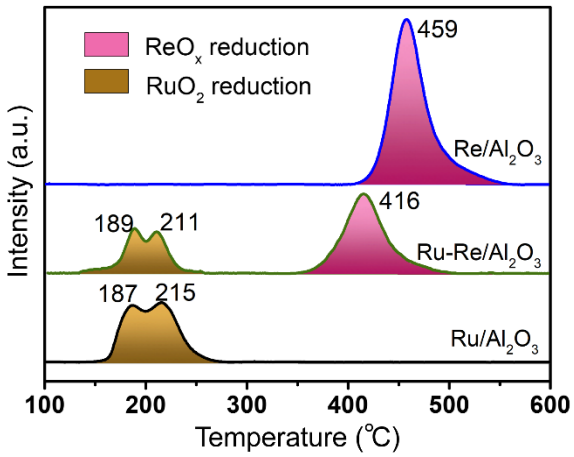

Figure 3. TPR profiles for prepared samples. Baselines have been corrected to remove periodic noise due to fluctuation of detector temperature.

In durability tests for 72 h, Ru-Re/Al_2O_3 slightly reduced its activity in 40 h and then became stable (Figure 4a). The spent catalyst contained only 0.4 wt% of coke, and we observed no deposit on the reactor wall below the catalyst bed, *viz.* no sublimation of Re. However, Re species partially aggregated as seen in the XRD pattern (26.2° ReO_2 (111); Figure 1b). STEM

analysis showed that Re species were in larger particle sizes of 1 to 3 nm (Figure 1d), compared to those on the unused catalyst (Figure 1c). Meanwhile, Ru did not undergo sintering (RuO_2 21 nm before reaction, Ru 21 nm after reaction; Figures 1a, b). Thus, the catalyst initially experiences growth of Re species and afterward it is stabilized. We have also found that the catalyst is stable with almost no coke formation (0.2 wt% at 72 h) under a stoichiometric ratio of $O_2/CH_4 = 0.5$ (Figure S5). In contrast, Ru/Al_2O_3 clearly decreased the catalytic activity after 10 h (Figure 4b), and possessed 3.0 wt% of coke on the catalyst. We conclude that the combination of Ru and Re provides higher activity for POM for a long time with less formation of coke, compared to Ru/Al_2O_3.

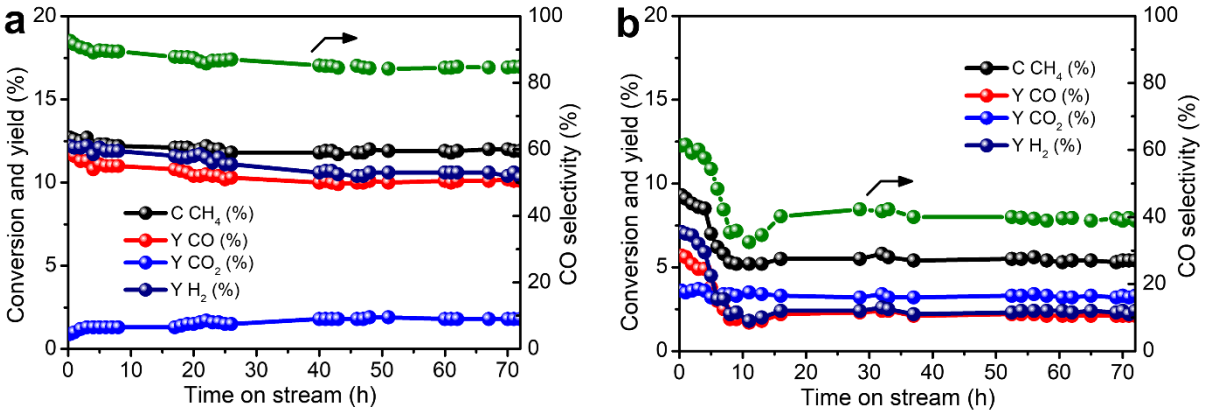

Figure 4. Durability test of (a) $Ru\text{-}Re/Al_2O_3$ and (b) Ru/Al_2O_3 in the POM reaction. Conditions: 600 °C, $CH_4:O_2:N_2$ = 50:4:46, SV = 120,000 mL g^{-1} h^{-1}, corresponding to W/F = 8.3×10^{-6} g h mL^{-1}.

Mechanistic study for direct partial oxidation

We studied effect of contact time (W/F, defined as the weight of catalyst per total flow rate of gases) on POM to clarify the reaction pathway for $Ru\text{-}Re/Al_2O_3$ and Ru/Al_2O_3. $Ru\text{-}Re/Al_2O_3$

produced CO in 52% selectivity and H_2 in 29% selectivity at 4.8% conversion of CH_4 at a very short contact time (3.3×10^{-7} g h mL^{-1}, corresponding to SV = 3,000,000 mL g^{-1} h^{-1}; Figure 5a, highlighted part), where O_2 was remaining (O_2 78% conv.). We further demonstrated formation of CO with 64% selectivity and H_2 with 57% selectivity at an earlier stage (CH_4 conv. 1.5%) by decreasing temperature to 500 °C (Table S3). As also discussed based on Figure 2 in the previous section, Re leads to the formation of CO in the presence of O_2. These results evidence the presence of direct partial oxidation pathway, because catalysts for the indirect pathway give almost no CO when O_2 is remaining.[22, 49, 50] After completely consuming O_2, the result approached a chemical equilibrium value given by SRM and RWGS (CO yield 15%, H_2 yield 15%) at a long contact time. Therefore, Ru-Re/Al_2O_3 can produce CO and H_2 without passing through complete oxidation, but the catalyst shows activity also for SRM and RWGS at a longer contact time. The former reaction, direct partial oxidation, is much faster than SRM and RWGS. For Ru/Al_2O_3, the catalyst gave a lower selectivity for CO (25%) at 3.4% conversion of CH_4 at the short contact time (3.3×10^{-7} g h mL^{-1}; Figure 5b). Moreover, CO was not produced at a further lower conversion of CH_4 (0.26%) at 500 °C (Table S3). After the complete consumption of O_2, the product distribution approached the chemical equilibrium in a slower rate than that of Ru-Re/Al_2O_3. Hence, Ru/Al_2O_3 catalyzes POM by the indirect pathway mostly, and the catalyst is less active than Ru-Re/Al_2O_3. A previous work also showed that Ru/Al_2O_3 promoted the indirect oxidation pathway.[22]

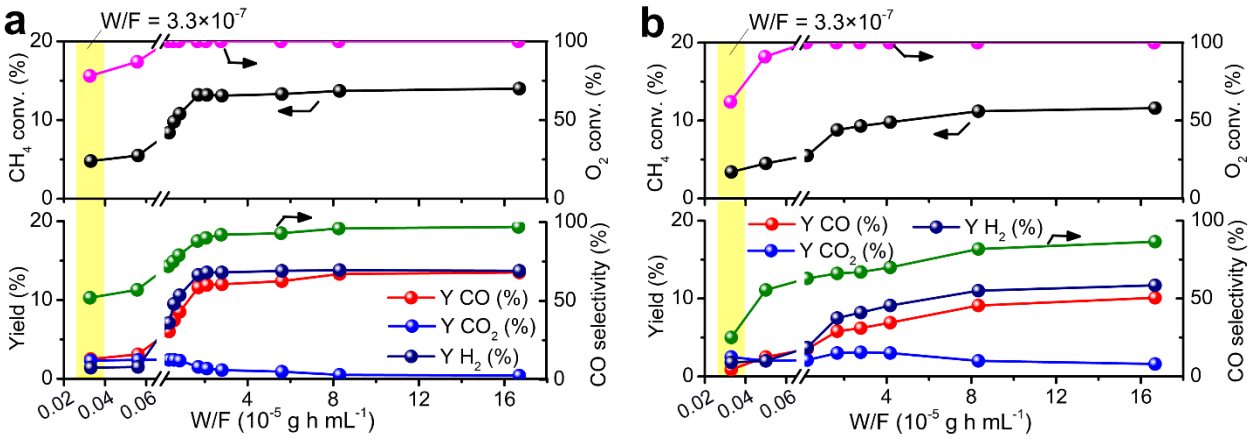

Figure 5. Effect of contact time on the POM over (a) Ru-Re/Al_2O_3 and (b) Ru/Al_2O_3. Reaction conditions: CH_4: O_2: N_2 = 50:4:46 at 600 °C.

In-situ diffuse reflectance infrared Fourier transform (DRIFT) was applied to unveil the intermediate for the direct partial oxidation pathway working on Ru-Re/Al_2O_3 (Figure 6). The background spectrum was measured after heat-treatment of the catalyst under He purge. Afterward, CH_4 was introduced on the catalyst at room temperature, followed by purge with He. Elevating temperature to 50 °C, adsorbed CH_4 was remaining as indicated by peaks at 3016 and 1305 cm^{-1} corresponding to stretching and bending of C–H.[54] By increasing the temperature to 100 and 150 °C, the CH_4 peak decreased, while peaks assignable to μ^2-type formate appeared at 1372 cm^{-1} (ν_s(OCO)), 1392 cm^{-1} (δ(CH)), 1586 cm^{-1} (ν_{as}(OCO)), and 2907 cm^{-1} ν(CH).[55-58] Low intensity of the ν(CH) peak is reasonable due to only small change in dipole moment by the stretch. The formate peaks other than that at 1392 cm^{-1} decreased by further increasing temperature and almost completely disappeared at 350 °C. The peak at 1392 cm^{-1} only became weaker and shifted to 1388 cm^{-1} during the period, perhaps due to overlap with peaks for carbonate species or sulfate on alumina.[59, 60] Therefore, we propose that most of formate species

are decomposed at 350 °C. Meanwhile, the increase in temperature produced a sharp peak at 1844 cm^{-1} and a broad peak at 1927 cm^{-1}, which were stretching of CO molecules adsorbed on hollow or bridge sites of metal.[61, 62] Another weak band was found at 1461 cm^{-1}, attributed to ν_{as}(OCO) of carbonate or ν_{s}(OCO) of carboxylate groups.[55, 63] The former is more probable due to low possibility of formation of C_2 or higher compounds at a low concentration of CH_4 in the system. These results suggest that CH_4 is converted to formate by using surface or lattice oxygen species, and the formate is eventually decomposed to CO and CO_2. Formate is sometimes found as a spectator in infrared spectroscopy for the conversion of C_1 compounds,[64] but this possibility can be excluded in our case. Because CH_4 was removed before formation of CO, only formate can be the source of CO under the experimental conditions. In contrast to Ru-Re/Al_2O_3, Ru/Al_2O_3 did not afford peaks for formate or CO under the same measurement conditions (Figure S6). The direct partial oxidation reaction likely takes place on ReO_x species. Produced CO may not adsorb on ReO_x species, but diffuses and adsorbs on Ru metal, which can be detected by the spectroscopy. Although the above mentioned results were obtained in the absence of O_2, we have observed the formation of formate on Ru-Re/Al_2O_3 also in CH_4/O_2 mixture, and consumption of the species after purging the system with He (Figures S7, S8).

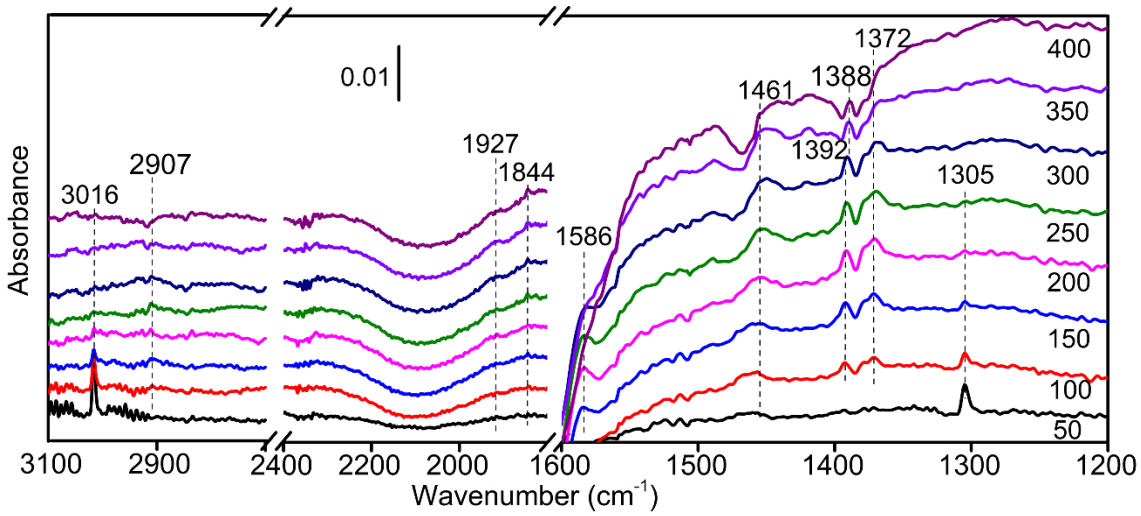

Figure 6. *In-situ* DRIFT spectra for temperature programmed reaction of CH_4 on Ru-Re/Al_2O_3. After background measurement, CH_4 was adsorbed and purged with He. Then, temperature was elevated by 10 °C min^{-1}.

To support the formate-intermediate hypothesis, decomposition of formic acid (Figure 7) was conducted using Ru-Re/Al_2O_3 at 600 °C, a typical temperature for POM. Vaporized formic acid was fed together with He carrier at a very high SV of 3,000,000 mL g^{-1} h^{-1} to minimize successive reactions of products. The catalyst produced CO in 65% selectivity and CO_2 in 35% selectivity, which was similar to the POM reaction at the same SV of 3,000,000 mL g^{-1} h^{-1} at 500 °C giving CO in 64% selectivity. Therefore, it is plausible that Re species converts CH_4 to formate and the intermediate decomposes to CO.

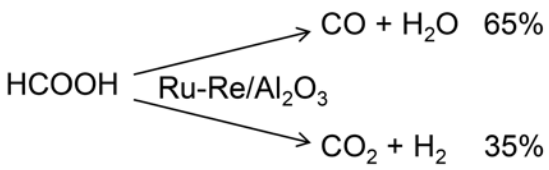

Figure 7. Decomposition of formic acid on Ru-Re/Al_2O_3 at 600 °C with an SV of 3,000,000 mL g^{-1} h^{-1}.

Effect of Re on indirect reaction pathway

To evaluate activity for the indirect pathway, SRM and RWGS reactions were carried out with Ru-Re/Al_2O_3 and monometallic catalysts at 600 °C.

For the SRM at CH_4:N_2 = 1:1 with water vapor (Table S4), CO yield was 7.6% (87% sel.) for Ru/Al_2O_3 and 9.5% (97% sel.) for Ru-Re/Al_2O_3. Re/Al_2O_3 was inactive for SRM (CO 0.16% yield) probably owing to the oxidized state of Re. Thus, the bimetallic catalyst shows the highest activity for SRM.

From the RWGS reactions at CO_2:H_2:Ar = 1:1:2 (Table S5), the three catalysts showed similar CO_2 conversion (37–38%) and CO selectivity (88–91%), and the remaining part was CH_4 (9–12% sel.). These results are similar to a thermodynamic equilibrium (CO_2 conv. 37%, CO sel. 95%, CH_4 sel. 5.4%), indicating that all the three catalysts are very active for this reaction. Re/Al_2O_3 was perhaps reduced to be active for RWGS without Ru under the very reducing ambient of RWGS.

Whole reaction pathway

We propose the whole reaction pathway on Ru-Re/Al_2O_3 based on all the analysis (Figure 8). First, Ru initiates the POM to CO and H_2 *via* the indirect pathway (Figure 8 left) as indicated by the activity of Ru/Al_2O_3 and the contact time study. The produced H_2 either in a form of gas

or spillover species reduces nearly-heptavalent Re to a lower valent ReO_x species such as ReO_2 as observed by XRD and STEM. XANES and TPR studies have supported the partial reduction of Re species. Afterward, the DRIFT study has shown that ReO_x species converts CH_4 to formate species ($CH_4 + 3O \rightarrow HCOO^- + H^+ + H_2O$) (Figure 8 center). In this reaction, we hypothesize water as the main coproduct, because the selectivity for H_2 is low at the initial stage (29% at W/F = 3.3×10^{-7} g h mL^{-1} at 600 °C). As for the O species, the measurement indicates that surface or lattice oxygen species on ReO_x can be used, and therefore a possible role of O_2 molecules is to regenerate the O species. Wang *et al.* reported Re_2O_7/SiO_2 catalyst active for the oxidation of CH_4 to formaldehyde at a similar temperature.[65] Our study suggests the partial reduction of Re significantly increases the activity for a one-step deeper oxidation of CH_4 to produce formate. The formate species is decomposed to $CO+H_2O$ and CO_2+H_2 in about 2:1 ratio. By increasing contact time, O_2 is completely consumed and then SRM and RWGS take place on both ReO_x and Ru (Figure 8 right). In this stage, Ru-Re/Al_2O_3 shows a higher activity than Ru/Al_2O_3 for SRM.

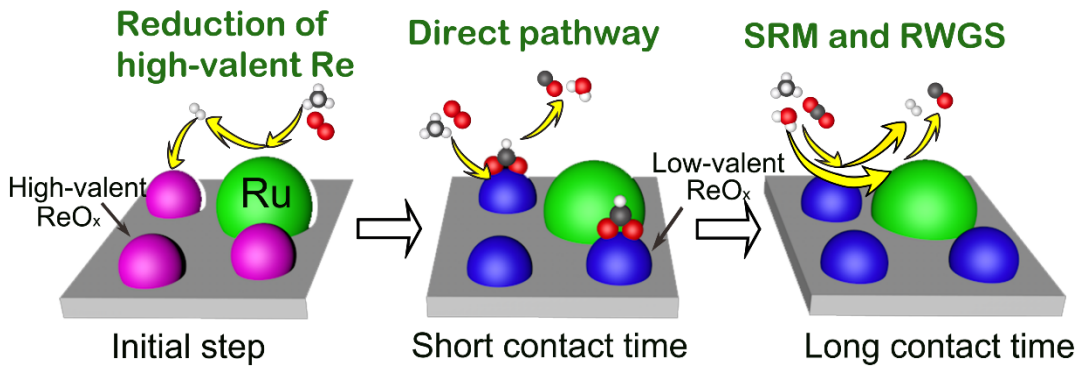

Figure 8. Scheme of POM over Ru-Re/Al_2O_3.

Conclusion

Bimetallic Ru-Re/Al_2O_3 catalyst was prepared and applied for POM reaction. The catalyst showed a greater activity than monometallic Ru or Re catalysts. The yields of CO and H_2 were increased up to 54% and 61%, respectively, under the reaction conditions of an O_2/CH_4 ratio of 0.5, SV = 60,000 mL g^{-1} h^{-1} and 600 °C. Controlled experiments and mechanistic study have shown that the main role of Ru is the reduction of Re species to a lower valent ReO_x. The *in-situ* produced Re species creates the direct partial oxidation pathway *via* formate intermediate, as evidenced by DRIFT and contact time studies. At a longer contact time, SRM and RWGS become predominant, catalyzed by Ru and ReO_x. Even though the POM contains the equilibrium reactions similar to the indirect pathway, this is a very rare case that demonstrated the presence of direct partial oxidation pathway. Moreover, the formate intermediate is different from the previous observations that atomic carbon is needed for producing CO. Our finding suggests a new catalyst design using Re not as a promoter but as a main active species especially towards production of CO *via* the direct partial oxidation of CH_4.

ASSOCIATED CONTENT

Supporting Information

Detailed information about catalyst characterization and activity tests, effects of metal loading amounts and supports on POM, STEM images, and *in-situ* DRIFT spectra.

AUTHOR INFORMATION

Corresponding Author

*E-mail: kobayashi.hi@cat.hokudai.ac.jp

Author Contributions

L.L., H.K., and A.F. wrote the manuscript. L.L. performed all experiments other than XANES measurements (A.S.) and RWGS reaction (N.H.MD.D.). H.K. conducted the project with advises of A.F. All authors have given approval to the final version of the manuscript.

Funding Sources

Cross-ministerial Strategic Innovation Promotion Program (SIP) organized by Cabinet Office, Government of Japan. Japan Science and Technology Agency (JST) CREST Grant Number JPMJCR15P4.

Notes

The authors declare no competing financial interest.

ACKNOWLEDGMENT

We would like to thank Dr. E. Kusumawati for preliminary TEM measurements, Ms. N. Hirai for taking the STEM images, and Prof. K. Asakura for assisting the XANES measurement. This work was partially supported by Cross-ministerial Strategic Innovation Promotion Program (SIP) organized by Cabinet Office, Government of Japan and by Japan Science and Technology Agency (JST) CREST Grant Number JPMJCR15P4.

REFERENCES

(1) Schüth, F. Making more from methane. *Science* **2019**, 363, 1282–1283.

(2) Pakhare, D.; Spivey, J. A review of dry (CO_2) reforming of methane over noble metal catalysts. *Chem. Soc. Rev.* **2014**, 43, 7813–7837.

(3) Zhu, J.; Wang, L.; Zuidema, E.; Mondal, K.; Zhang, M.; Zhang, J.; Wang, C.; Meng, X.; Yang, H.; Mesters, C.; Xiao, F. Hydrophobic zeolite modification for in situ peroxide formation in methane oxidation to methanol. *Science* **2020**, 367, 193–197.

(4) Schwach P.; Pan, X.; Bao, X. Direct conversion of methane to value-added chemicals over heterogeneous catalysts: challenges and prospects. *Chem. Rev.* **2017**, 117, 8497–8520.

(5) Ravi, M.; Ranocchiari M.; Bokhoven, J. A. V. The direct catalytic oxidation of methane to methanol-a critical assessment. *Angew. Chem., Int. Ed.* **2017**, 56, 16464–16483.

(6) Li, Y. K.; Yuan, Z.; Zhao, Y. X.; Zhao, C.; Liu, Q. Y.; Chen H.; He, S. G. Thermal Methane Conversion to Syngas Mediated by Rh_1-Doped Aluminum Oxide Cluster Cations $RhAl_3O_4$. *J. Am. Chem. Soc.* **2016**, 138, 12854–12860.

(7) Olivos-Suarez, A. I.; Szécsényi, À.; Hensen, E. J. M.; Ruiz-Martinez, J.; Pidko, E. A.; Gascon, J. Strategies for the direct catalytic valorization of methane using heterogeneous catalysis: challenges and opportunities. *ACS Catal.* **2016**, 6, 2965–2981.

(8) Vogt, C.; Kranenborg, J.; Monai M.; Weckhuysen, B. M. Structure sensitivity in steam and dry methane reforming over nickel: activity and carbon formation. *ACS Catal*. **2019**, 10, 1428–1438.

(9) Rostrup-Nielsen, J. R. Sulfur-passivated nickel catalysts for carbon-free steam reforming of methane. *J. Catal.* **1984**, 85, 31–43.

(10) Enger, B. C.; Lødeng R.; Holmen, A. A review of catalytic partial oxidation of methane to synthesis gas with emphasison reaction mechanisms over transition metal catalysts. *Appl.Catal. A* **2008**, 346, 1–27.

(11) Shafiefarhood, A.; Zhang, J.; Neal, L. M.; Li, F. Rh-promoted mixed oxides for "low-temperature" methane partial oxidation in the absence of gaseous oxidants. *J. Mater. Chem. A* **2017**, 5, 11930–11939.

(12) Hou, Y.; Nagamatsu, S.; Asakura, K.; Fukuoka, A.; Kobayashi, H. Trace mono-atomically dispersed rhodium on zeolite-supported cobalt catalyst for the efficient methane oxidation. *Commun. Chem.* **2018**, 1, 41.

(13) Yasuda, S.; Osuga, R.; Kunitake, Y.; Kato, K.; Fukuoka, A.; Kobayashi, H.; Gao, M.; Hasegawa, J.; Manabe, R.; Shima, H.; Tsutsuminai, S.; Yokoi, T. Zeolite-supported ultra-small nickel as catalyst forselective oxidation of methane to syngas. *Commun. Chem.* **2020**, 3, 129.

(14) Liu, Y.; Qin, L.; Cheng, Z.; Goetze, J. W.; Kong, F.; Fan J. A.; Fan, L. S. Near 100% CO selectivity in nanoscaled iron-based oxygen carriers for chemical looping methane partial oxidation. *Nat. Commun.* **2019**, 10, 5503.

(15) Osman, A. I. Catalytic hydrogen production from methane partial oxidation: mechanism and kinetic study. *Chem. Eng. Technol.* **2020**, 43, 641–648.

(16) Kondratenko, V. A.; Berger-Karin, C.; Kondratenko, E. V. Partial oxidation of methane to syngas over γ-Al_2O_3-supported Rh nanoparticles: kinetic and mechanistic origins of size effect on selectivity and activity. *ACS Catal.* **2014**, 4, 3136−3144.

(17) Zhu, Y.; Zhang, S.; Shan, J.; Nguyen, L.; Zhan, S.; Gu, X.; Tao F. In situ surface chemistries and catalytic performances of ceria doped with Palladium, Platinum, and Rhodium in methane partial oxidation for the production of syngas. *ACS Catal.* **2013**, 3, 2627−2639.

(18) Campaa, M.C.; Ferrarisa, G.; Gazzolib, D.; Pettitib, I.; Pietrogiacomi, D. Rhodium supported on tetragonal or monoclinic ZrO_2 as catalyst for the partial oxidation of methane. *Appl. Catal. B.* **2013**, 142–143, 423– 431.

(19) Ciminoa, S.; Mancinob, G.; Lisi L. Sulphur tolerance of a P-doped Rh/-Al_2O_3 catalyst during the partial oxidation of methane to syngas. *Appl. Catal. B.* **2013**, 138–139, 342– 352.

(20) Scarabello, A.; Nogare, D. D.; Canu, P.; Lanza, R. Partial oxidation of methane on Rh/ZrO_2 and Rh/Ce–ZrO_2 on monoliths: Catalyst restructuring at reaction conditions. *Appl. Catal. B.* **2015**, 174–175, 308–322.

(21) Das, S.; Gupta, R.; Kumar, A.; Shah, M.; Sengupta, M.; Bhandari, S.; Bordoloi, A. Facile synthesis of Ruthenium decorated $Zr_{0.5}Ce_{0.5}O_2$ nanorods for catalytic partial oxidation of methane. *ACS Appl. Nano Mater.* **2018**, 1, 2953−2961.

(22) Goodman, E. D.; Latimer, A. A.; Yang, A.-C.; Wu, L.; Tahsini, N.; Frank Abild-Pedersen, F.; Cargnello, M. Low-Temperature Methane Partial Oxidation to Syngas with Modular Nanocrystal Catalysts. *ACS Appl. Nano Mater.* **2018**, 1, 5258-5267.

(23) Choque, V.; Homs, N.; Cicha-Szot, R.; Piscina, P. R. Study of ruthenium supported on Ta_2O_5–ZrO_2 and Nb_2O_5–ZrO_2 as catalysts for the partial oxidation of methane. *Catal. Today* **2009**,142, 308–313.

(24) Balint, I.; Miyazaki, A.; Aika, K. The relevance of Ru nanoparticlesmorphology and oxidation state to the partial oxidation of methane. *J. Catal.* **2003**, 220, 74–83.

(25) Weng, W. Z.; Chen, M. S.; Yan, Q. G.; Wu, T. H.; Chao, Z. S.; Liao, Y. Y.; Wan, H. L. Mechanistic study of partial oxidation of methane to synthesis gas over supported rhodium and ruthenium catalysts using in situ time-resolved FTIR spectroscopy. *Catal. Today* **2000**, 63, 317–326.

(26) Yoo, J. S.; Schumann, J.; Studt, F.; Abild-Pedersen, F.; Nørskov, J. K. Theoretical investigation of methane oxidation on Pd(111) and other metallic surfaces. *J. Phys. Chem. C* **2018**, 122, 16023−16032.

(27) Siang, T. J.; Jalil, A. A.; Hamid, M. Y. S.; Abdulrasheed, A. A.; Abdullah, T. A. T.; Vo, D. V. N. Role of oxygen vacancies in dendritic fibrous M/KCC-1 (M = Ru, Pd, Rh) catalysts for methane partial oxidation to H_2-rich syngas production. *Fuel* **2020**, 278, 118360.

(28) Luo, Z.; Kriz, D. A.; Miao, R.; Kuo, C. H.; Zhong, W.; Guild, C.; He, J.; Willis, B.; Dang, Y.; Suib, S. L.; Nandi P. TiO_2 Supported gold–palladium catalyst for effective syngas production from methane partial oxidation. *Appl. Catal. A* **2018**, 554, 54–63.

(29) Araújo, J. C. S.; Oton, L. F. Bessa, B.; Neto, A. B. S.; Oliveira, A. C.; Lang, R.; Otubo, L.; Bueno, J. M. C. The role of Pt loading on La_2O_3-Al_2O_3 support for methane conversion reactions via partial oxidation and steam reforming. *Fuel* **2019**, 254, 115681.

(30) Ma, L.; Ding, C.; Wang, J.; Li, Y.; Xue, Y.; Guo, J.; Zhang, K.; Liu, P.; Gao, X. Highly dispersed Pt nanoparticles confined within hierarchical pores of silicalite-1 zeolite via crystal

transformation of supported Pt/S-1 catalyst for partial oxidation of methane to syngas. *Int. J. Hydrogen Energ.* **2019**, 44, 21847–21857.

(31) Boukha, Z.; Jiménez-González, C.; Rivas, B.; González-Velasco, J. R.; Gutiérrez-Ortiz, J. I.; López-Fonseca, R. Synthesis, characterisation and performance evaluation of spinel-derived Ni/Al_2O_3 catalysts for various methane reforming reactions. *Appl. Catal. B* **2014**, 158–159, 190–201.

(32) Chalupka, K. A.; Jozwiak, W. K.; Rynkowski, J.; Maniukiewicz, W.; Casale, S.; Dzwigaj, S. Partial oxidation of methane on Ni_xAlBEA and Ni_xSiBEA zeolite catalysts: Remarkable effect of preparation procedure and Ni content. *Appl. Catal. B* **2014**, 146, 227–236.

(33) Gil-Calvo, M.; Jiménez-González, C.; Rivas, B.; Gutiérrez-Ortiz, J. I.; López-Fonseca, R. Effect of Ni/Al molar ratio on the performance of substoichiometric $NiAl_2O_4$ spinel-based catalysts for partial oxidation of methane. *Appl. Catal. B* **2017**, 209, 128–138.

(34) Osman, A. I.; Meudal, J.; Laffir, F.; Thompson, J.; Rooney, D. Enhanced catalytic activity of Ni on η-Al_2O_3 and ZSM-5 on addition of ceria zirconia for the partial oxidation of methane. *Appl. Catal. B* **2017**, 212, 68–79.

(35) Pantaleo, G.; Parola, V. L.; Deganello, F.; Calatozzo, P.; Bal, R.; Venezia, A. M. Synthesis and support composition effects on CH_4 partial oxidation over Ni–CeLa oxides. *Appl. Catal. B* **2015**,164, 135–143.

(36) Antaleo, G.; Parola, V. L.; Deganello, F.; Singha, R. K.; Bal, R.; Venezia, A. M. Ni/CeO_2 catalysts for methane partial oxidation: Synthesis driven structural and catalytic effects. *Appl. Catal. B* **2016**,189, 233–241.

(37) Singha, R. K.; Shukla, A.; Yadav, A.; Konathala, L. N. S.; Bal, R. Effect of metal-support interaction on activity and stability of Ni-CeO_2 catalyst for partial oxidation of methane. *Appl. Catal. B* **2017**, 202, 473–488.

(38) Benito, P.; Santo, V. D.; Grandi, V. D. Marelli, M.; Fornasaria, G.; Psaro, R.; Vaccari, A. Coprecipitation versus chemical vapour deposition to prepare Rh/Ni bimetallic catalysts. *Appl. Catal. B* **2015**, 179, 150–159.

(39) Lanza, R.; Canu, P.; Järås, S. G. Partial oxidation of methane over Pt–Ru bimetallic catalyst for syngas production. *Appl. Catal. A* **2008**, 348, 221–228.

(40) Figen, H. E.; Baykara, S. Z. Effect of ruthenium addition on molybdenum catalysts for syngas production via catalytic partial oxidation of methane in a monolithic reactor. *Int. J. Hydrogen Energ.* **2018**, 43, 1129–1138.

(41) Velasco, J. A.; Fernandez, C.; Lopez, L.; Cabrera, S.; Boutonnet, M.; Järås, S. Catalytic partial oxidation of methane over nickel and ruthenium based catalysts under low O_2/CH_4 ratios and with addition of steam. *Fuel* **2015**, 153, 192–201.

(42) Branco, J. B.; Ferreira, A. C.; Gasche, T. A.; Pimenta, G.; Leal, J. P. Low temperature partial oxidation of methane over bimetallic nickel-*f* block element oxide nanocatalysts. *Adv. Synth. Catal.* **2014**, 356, 3048–3058.

(43) Li, L.; Lu, P.; Yao, Y.; Ji, W. Silica-encapsulated bimetallic Co–Ni nanoparticles as novel catalysts for partial oxidation of methane to syngas. *Catal. Commun.* **2012**, 26, 72–77.

(44) Maniecki, T. P.; Stadnichenko, A. I.; Maniukiewicz, W.; Bawolak, K.; Mierczyński, P.; Boronin, A. I.; Jozwiak, W. K. An active phase transformation on surface of Ni-Au/Al_2O_3 catalyst during partial oxidation of methane to synthesis gas. *Kinet. Catal.* **2010**, 51, 573–578.

(45) K. Bawornruttanaboonya, N. Laosiripojana, A. S. Mujumdar and S. Devahastin, Catalytic partial oxidation of CH_4 over bimetallic Ni-Re/Al_2O_3: kinetic determination for application in microreactor. *AIChE J.* **2018**, 64, 1691–1701.

(46) Cheephat, C.; Daorattanachai, P.; Devahastin S.; Laosiripojana, N. Partial oxidation of methane over monometallic and bimetallic Ni-, Rh-, Re- based catalysts: Effects of Re addition, co-fed reactants and catalyst support. *Appl. Catal. A* **2018**, 563, 1–8.

(47) Prettre, M.; Eichner, C.; Perrin, M. The catalytic oxidation of methane to carbon monoxide and hydrogen. *Trans. Faraday Soc.* **1946**, 42, 335–339.

(48) York, A. P. E.; Xiao, T.; Green, M. L. H. Brief overview of the partial oxidation of methane to synthesis gas. *Top. Catal.* **2003**, 22, 345–358.

(49) Looij, F. V.; Stobbe, E. R.; Geus, J. W. Mechanism of the partial oxidation of methane to synthesis gas over Pd. *Catal. Lett.* **1998**, 50, 59–67.

(50) Hou, Y.; Ogasawara, S.; Fukuoka A.; Kobayashi, H. Zeolite-supported rhodium sub-nano cluster catalyst for low-temperature selective oxidation of methane to syngas. *Catal. Sci. Technol.* **2017**, 7, 6132–6139.

(51) Elmasides, C.; Verykios, X. E.; Mechanistic study of partial oxidation of methane to synthesis gas over modified Ru/TiO_2 catalyst. *J. Catal.* **2001**, 203, 477–486.

(52) Nakagawa, Y.; Tazawa, S.; Wang, T.; Tamura, M.; Hiyoshi, N.; Okumura K.; Tomishige, K. Mechanistic study of hydrogen-driven deoxydehydration over ceria-supported rhenium catalyst promoted by Au nanoparticles. *ACS Catal.* **2017**, 8, 584–595.

(53) Im, J.; Shin, H.; Jang, H.; Kim H.; Choi, M. Maximizing the catalytic function of hydrogen spillover in platinum-encapsulated aluminosilicates with controlled nanostructures. *Nat. Commun.* **2014**, 5, 3370.

(54) Li, C.; Li, G.; Xin, Q. FT-IR spectroscopic studies of methane adsorption on magnesium oxide. *J. Phy. Chem.* **1994**, 98, 1933–1938.

(55) Betta, R. A. D.; Shelef, M. Heterogeneous methanation: In situ infrared spectroscopic study of $RuAl_2O_3$ during the hydrogenation of CO. *J. Catal.* **1977**, 48, 111–119.

(56) Busca, G.; Lamotte, J.; Lavalley, J. C.; Lorenzelli, V. FT-IR study of the adsorption and transformation of formaldehyde on oxide surfaces. *J. Am. Chem. Soc.* **1987**, 109, 5197–5202.

(57) Falbo, L.; Visconti, C. G.; Lietti, L.; Szanyi, J. The effect of CO on CO_2 methanation over Ru/Al_2O_3 catalysts: a combined steady-state reactivity and transient DRIFT spectroscopy study. *Appl. Catal. B.* **2019**, 256, 117791.

(58) Li, X.; Li, L.; Lin, J.; Qiao, B.; Yang, X.; Wang, A.; Wang, X. Reactivity of Methanol Steam Reforming on ZnPd Intermetallic Catalyst: Understanding from Microcalorimetric and FT-IR Studies. *J. Phys. Chem. C* **2018**, 122, 12395–12403.

(59) Jodłowski, P. J.; Je˛drzejczyk, R. J.; Chlebda, D.; Gierada, M.; Łojewska, J. In situ spectroscopic studies of methane catalytic combustion over Co, Ce, and Pd mixed oxides deposited on a steel surface. *J. Catal.* **2017**, 350, 1–12.

(60) Wilburn, M. S.; Epling, W. S. SO_2 adsorption and desorption characteristics of bimetallic Pd-Pt catalysts: Pd:Pt ratio dependency. *Catal. Today* **2019**, 320, 11–19.

(61) Ekerdt, J. G.; Bell, A. T. Synthesis of hydrocarbons from CO and H_2 over silica-supported Ru: Reaction rate measurements and infrared spectra of adsorbed species. *J. Catal.* **1979**, 58, 170–187.

(62) Tada, S.; Kikuchi, R. Mechanistic study and catalyst development for selective carbon monoxide methanation. *Catal. Sci. Technol.* **2015**, 5, 3061–3070.

(63) Datka, J.; Sarbak, Z.; Eischens, R. Infrared study of coke on alumina and zeolite. *J. Catal.* **1994**, 145, 544–550.

(64) Li, X.; Lin, J.; Li, L.; Huang, Y.; Pan, X.; Collins, S. E.; Ren, Y.; Su, Y.; Kang, L.; Liu, X.; Zhou, Y.; Wang, H.; Wang, A.; Qiao, B.; Wang, X.; Zhang, T. Controlling CO_2 Hydrogenation Selectivity by Metal-Supported Electron Transfer. *Angew. Chem., Int. Ed.* **2020**, 59, 19983–19989.

(65) Wang, Y.; Otsuka, K.; Wan, H.; Partial oxidation of methane and ethane to oxygenates over silica supported rhenium oxide. *React. Kinet. Catal. Lett.* **2003**, 79, 127–133.

Table of Contents

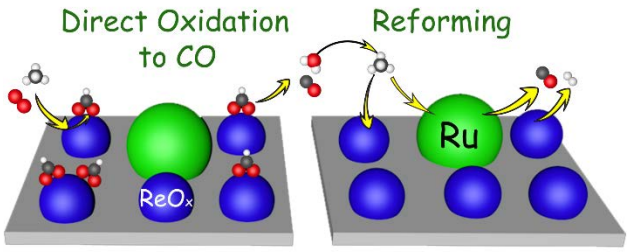
Direct Oxidation
to CO
Reforming
ReOx
Ru